








# Verification of the Existence of Recently Published New Energy Levels of Atomic Holmium

D. Bingöl<sup>1</sup> , Gö. Başar<sup>2\*</sup> , Gü. Başar<sup>3</sup> , I. K. Öztürk<sup>2</sup> , F. Güzelçimen<sup>2</sup> , S. K. Barka<sup>4,5</sup> , and S. Kröger<sup>6</sup> 

<sup>1</sup>Istanbul University, Institute of Graduate Studies in Sciences, 34452, Beyazit, Istanbul, Türkiye

<sup>2</sup>Istanbul University, Faculty of Science, Department of Physics, 34134, Vezneciler, Istanbul, Türkiye

<sup>3</sup>Istanbul Technical University, Faculty of Science and Letters, Physics Engineering Department, 34469, Maslak, Istanbul, Türkiye

<sup>4</sup>Istanbul Technical University, Graduate School, Physics Engineering Program, 34469, Maslak, Istanbul, Türkiye

<sup>5</sup>Acibadem Mehmet Ali Aydınlar University, Vocational School of Health Services, Opticianry Program, 34752, Ataşehir, Istanbul, Türkiye

<sup>6</sup>Hochschule für Technik und Wirtschaft Berlin, Fachbereich 1, Wilhelminenhofstr. 75A, 12459, Berlin, Germany

## ABSTRACT

The objective of this work was to review five energy levels of atomic Holmium that are reported in the literature, for which are indicated that further verification is required. All theoretically possible transitions to these 5 levels were investigated experimentally in the wavelength region of a TiSa laser from 693 nm to 765 nm using laser-induced fluorescence spectroscopy and a hollow cathode discharge lamp. In case a laser-induced fluorescence was detected, the hyperfine structure of the measured lines was fitted and used as fingerprint in the confirmation of the levels under investigation. A total of 20 lines were investigated with laser spectroscopy, but only 2 among those lines were suitable for the intended verification. Therefore, selected lines from a previously measured Fourier Transform (FT) spectra were analysed, additionally. The experimental hyperfine structures were compared with the simulated ones. 9 of the 25 examined FT lines confirm the existence of the levels under investigation. Further 3 FT lines were strongly disturbed by neighbouring overlapped lines. Despite the number of lines, only 2 of 5 levels could be confirmed with high certainty. For the other 3 levels, the lines seen in the FT spectrum were either weak or unresolved, so that confirmation was not possible with a high degree of certainty.

**Keywords:** laser spectroscopy; hyperfine structure; holmium

## 1. INTRODUCTION

The rare earth element holmium (Ho), has an atomic number of 67 and has only one stable isotope, <sup>165</sup>Ho. It plays an important role in astrophysics, namely in the study of nucleosynthesis, the process by which heavy elements are created in stars, and in measuring the age of a star cluster (see for example, [Snedden et al. 2009](#)).

The ground state electron configuration of atomic holmium (Ho I) is [Xe]4f<sup>11</sup> 6s<sup>2</sup> with the term <sup>4</sup>I<sub>15/2</sub>. The isotope <sup>165</sup>Ho has the nuclear spin quantum number  $I = 7/2$ , relatively high nuclear magnetic moment  $\mu_I = 4.17(3) \mu_N$  and a fairly big electric quadrupole moment  $Q = +2.74$  barn - 3.6 barn ([Stone 2005](#)). Due to the open *f*-electron shell configuration, Ho I has a high density of spectral lines and a correspondingly large number of fine structure levels. All the mentioned properties distinguish Ho as a good candidate for the investigation of fine structure and hyperfine structure and make it a subject of study by us and other research groups, especially in the last decade ([Al-Labady et al. 2017](#); [Başar et al. 2017](#); [Stefanska et](#)

[al. 2018a,b,c](#); [Furmann et al. 2018](#); [Özdağlıç et al. 2019a,b,c](#); [Elantkowska et al. 2019](#); [Başar et al. 2020](#); [Chomski et al. 2021, 2022, 2023](#)). Despite all accomplished and ongoing research, there is still lack of information on the fine structure (fs) and hyperfine structure (hfs) of Ho I.

In the most recent paper on the fs and hfs of atomic Ho conducted by [Chomski et al. \(2023\)](#), 32 new energy levels are given. It is stated by [Chomski et al. \(2023\)](#) that five of these levels need further verification. The purpose of the present study is to investigate and confirm these five levels.

## 2. EXPERIMENT

Laser induced fluorescence (LIF) spectroscopy was used to verify the unconfirmed energy levels of the Holmium atom given by [Chomski et al. \(2023\)](#). A laboratory made hollow cathode lamp was used to measure the hfs spectra of free Ho atoms. A 0.125 mm thick Ho foil was placed inside the 20 mm long cylindrical hollow cathode made of copper. The gas discharge

**Corresponding Author:** Gö. Başar **E-mail:** gbasar@istanbul.edu.tr

**Submitted:** 13.10.2023 • **Revision Requested:** 28.10.2023 • **Last Revision Received:** 05.11.2023 • **Accepted:** 06.11.2023



This article is licensed under a Creative Commons Attribution-NonCommercial 4.0 International License (CC BY-NC 4.0)

runs with Ne inert gas at about 2 mbar pressure and a discharge current of 60 mA. Doppler line broadening was reduced by cooling the cathode with liquid nitrogen.

A tunable cw single longitudinal mode Ti-Sa laser (Coherent, MBR 110, 4 W) pumped with a solid state laser (Coherent, Verdi 18 W) was used for the excitation of Ho atoms. In this study, the wavelength range from 693 nm to 765 nm was available. In order to keep the saturation broadening of the absorption lines low, the power of the laser was reduced to 1 W.

The laser beam was modulated with a mechanical chopper before passing through the gaseous plasma and the LIF measurements were performed with the lock-in technique. For the LIF measurements, the fluorescent light emitted from the hollow cathode lamp was collected with the help of a lens and mirrors and with another lens it was to be redirected and focused on the entrance slit of a monochromator (McPherson 607, grating: 1200 lines/mm). The fluorescence light was detected with a Photomultiplier (Hamamatsu, R928) at the exit slit of the monochromator. The fluorescence transitions from the upper level of the laser-excitation transition were recorded as positive LIF signals, whereas the fluorescence transitions from the lower level of the laser-excitation transition were recorded as negative LIF signals.

To measure the hfs of the lines under investigation, the laser wavelength was scanned continuously over a range of up to 25 GHz according to the width of the structures. The absolute wavelength of the laser was measured with the help of a wavemeter (High Finesse 6-200). For calibration of the relative frequency axis of the scan range, a small portion of the laser beam was sent to a lab-built, temperature-controlled confocal Fabry-Perot interferometer. The interference maxima obtained simultaneously with the measurement were used for the calibration of the frequency scale. The scanning rate of the wavelength was usually set to  $2.5 \text{ GHz min}^{-1}$  and recorded as steps of about 2 MHz. Each line measured with LIF was registered at least five times.

In addition to the laser measurements, data from Fourier Transform (FT) spectra were available for evaluation. The FT spectra in the wavelength range of 300 nm to 850 nm were measured with a resolution of  $0.025 \text{ cm}^{-1}$  with the FT Spectrometer IFS125 HR at the Laser Centre of the University of Latvia in Riga and were already discussed in our previous studies (Özdoğan et al. 2019a,b,c).

### 3. METHOD FOR INVESTIGATION OF UNCONFIRMED LEVELS

In this work, five fine structure energy levels indicated as “probably existing new” and “require further verification” by Chomski et al. (2023) were investigated for confirmation. These levels are listed in Table 1 together with all the information provided in the reference. The last column of Table 1 presents the result of our investigation, which will be explained in the following sections.

**Table 1.** Energy levels (sorted by parity and then by energy) given by Chomski et al. (2023) as new but unconfirmed, together with their  $J$  quantum number, parity  $p$  and hyperfine structure constants  $A$  and  $B$  as given in Chomski et al. (2023). For comment see text in Section 4.

$E(\text{cm}^{-1})$	$J$	$p$	$A$ (MHz)	$B$ (MHz)	Comment (this work)
39019.06	11/2	e	1111.8 (6.5)	231 (26)	confirmed
40438.59	13/2	e	784.8 (2.0)	388 (91)	further verification recomm.
42189.40	9/2	e	451.4 (1.4)	-698 (192)	further verification recomm.
36071.92	19/2	o	980.6 (1.5)	2043 (103)	confirmed
44283.99	23/2	o	619.3 (1.9)	2481 (113)	further verification recomm.

As a first step, all theoretically possible transitions to these five levels in the wavelength range of the laser were calculated. For this step the program ELEMENTS (Windholz 2016) was used. The programme allows to simulate the hfs of the lines and to search for the appropriate fluorescence lines. The simulations are based on the hfs constants  $A$  and  $B$  from the literature.

In the next step, for each line the laser was scanned at the position of the calculated wavelengths. The width of the scan was estimated by the results of the simulation of the hfs. For these LIF measurements, the monochromator was in each case adjusted to the most intense fluorescence lines from the lower or the upper energy levels of the calculated transition, respectively. Information about the intensities of the calculated fluorescence lines could be found in the literature (Özdoğan et al. 2019a,b) and was also provided via the program ELEMENTS. If no signal was found in the first attempt, other fluorescence lines were tested.

If a signal was detected and the line could be measured, subsequently the hfs of this line was examined. For this purpose the FITTER program (Zeiser et al. 2022) was used to fit the calculated hfs line profile to the experimental intensity distribution. The Voigt profile function was chosen. The program performs an iterative least-squares fit to optimize the fit parameters.

The focus of this present work is to confirm the findings of Chomski et al. (2023), for this to accomplish the HFS constants  $A$  and  $B$  of the upper and lower levels were fixed during the fit. The Voigt profile function with same profile parameter was used for each individual hfs component. The only free fit parameters were the centre of gravity of the hyperfine structure, the total intensity of the line, the full width at half maximum (FWHM) and a profile parameter, which describes the ratio of the Gaussian to the Lorentzian part in the Voigt profile. The intensities of the individual hfs components were coupled to the most intense component. Since in the LIF spectra the saturation effect clearly influences the intensity ratios of the individual hfs component, the saturation effect was taken into account, according to the procedure described in Kröger et al. (2023).

**Table 2.** Investigated energy levels, sorted by parity and energy together with all lines investigated with laser induced fluorescence (LIF) spectroscopy or Fourier transform (FT) spectroscopy. The second to last column lists the measurement method used in this work, the column before lists the method used in reference [1]. For comments see table notes.

Upper level from [1]			Line			Lower level			Comments		
$E$ (cm <sup>-1</sup> )	$J$	$p$	$\lambda_{\text{air}}$ (nm)	$\sigma$ (cm <sup>-1</sup> )	S/R	$E$ (cm <sup>-1</sup> )	$J$	$p$	[1]	This work	
39019.06(0.03)	11/2	e	496.102	20151.52		18867.54	13/2	o	LIF	FT	different structure
			527.327	18958.30	10	20060.76	11/2	o	LIF	FT*	observed
			539.653	18525.29	11	20493.77	13/2	o	observed	FT*	observed
			745.920	13402.58		25616.48	11/2	o		LIF*	observed
			756.564	13214.02		25805.04	9/2	o		LIF	different structure
40438.59(0.04)	13/2	e	457.196	21866.31		18572.28	15/2	o	FT	FT	different structure
			472.421	21161.65	7	19276.94	15/2	o	FT	FT**	blend
			501.243	19944.83		20493.76	13/2	o	LIF	FT	different structure
			533.023	18755.69	21	21682.90	15/2	o	observed	FT**	blend with very strong line (S/N=3900)
			542.606	18424.47	6	22014.12	15/2	o		FT*	observed, but very weak and only one peak
			557.880	17920.04	5	22518.55	11/2	o		FT**	only faintly visible at under a blending line
			693.527	14415.07		26023.52	15/2	o		LIF	not observed
			698.552	14311.37		26127.22	13/2	o		LIF	not observed
			702.044	14240.20		26198.39	15/2	o		LIF	not observed
			703.395	14212.84		26225.75	13/2	o		LIF	not observed
			706.494	14150.49		26288.10	13/2	o		LIF	not observed
			714.321	13995.46		26443.13	11/2	o		LIF	not observed
			715.015	13981.87		26456.72	15/2	o		LIF	not observed
			718.773	13908.76		26529.83	11/2	o		LIF	not observed
			725.810	13773.92		26664.67	11/2	o		LIF	not observed
			726.287	13764.87		26673.72	13/2	o		LIF	not observed
			733.621	13627.27		26811.32	15/2	o		LIF	not observed
739.650	13516.19		26922.40	15/2	o		LIF	not observed			
742.668	13461.25		26977.34	13/2	o		LIF	not observed			
746.688	13388.79		27049.80	11/2	o		LIF	not observed			
42189.40(0.05)	9/2	e	451.776	22128.64		20060.76	11/2	o	weak	FT	not observed
			499.074	20031.52	23	22157.88	9/2	o	LIF	FT*	observed
			508.226	19670.81	12	22518.59	11/2	o	LIF	FT	blend, no statement possible
			510.169	19595.87	4	22593.53	11/2	o	LIF	FT	very weak, other structure
			538.165	18576.48		23612.92	11/2	o	weak	FT	not observed
			737.989	13546.61		28642.79	11/2	o		LIF	not observed
764.707	13073.30		29116.10	11/2	o		LIF	not observed			
36071.92(0.05)	19/2	o	360.999	27693.01	9	8378.91	17/2	e	weak	FT	different structure
			403.933	24749.61	23	11322.31	21/2	e	FT	FT*	observed
			410.020	24382.15	178	11689.77	19/2	e	strong	FT*	observed, blend
			515.629	19388.40	14	16683.52	19/2	e	LIF	FT	different structure
			735.360	13595.03		22476.89	17/2	e		LIF	not observed
757.059	13205.37		22866.55	19/2	e		LIF*	observed			
44283.99(0.09)	23/2	o	438.683	22789.10		21494.89	21/2	e	observed	FT	not observed
			448.238	22303.32	4	21980.67	23/2	e	observed	FT*	observed, very weak
			477.940	20917.28	26	23366.71	21/2	e	FT	FT*	observed, blend
			478.136	20908.71	18	23375.28	25/2	e	observed	FT	blend
			493.013	20277.76	12	24006.23	23/2	e	LIF	FT	blend
			510.853	19569.65	19	24714.34	21/2	e	LIF	FT*	observed
			533.500	18738.92		25545.07	21/2	e	LIF	FT	not observed

there is no theoretical line to this level in the wavelength range used with our laser

[1] Chomski et al. (2022)

Note: p: parity, e: even, o: odd;

(\*): line used for confirmation; (\*\*): line with blend, confirmation not certain.

All comments in the third last column are from reference [1]; LIF not observed: the line is even not visible in our FT spectrum; different structure: the line is not observed, but another line is present at nearly the same wavelength

In addition to the laser measurements, lines were examined in the FT spectrum. For this as well the program ELEMENTS was used. All theoretically possible lines connected to the five levels under investigation were checked. If a signal was visible in the experimental FT spectrum, the hfs of the line was simulated and the simulated curve was compared with the corresponding section of the experimental spectrum. In several cases the line of interest was overlapped by another line (so-called blends). Sometimes the structure you are looking for can still be clearly recognised. Then the recognised section is compared with the simulation. Sometimes no clear statement can be made at all. In two cases the simulation was carried out with the superposition of two structures, in order to provide a better evidence for the investigated line. Since the simulation of the superposition of two structures is not possible with the simulation tool of the program ELEMENTS, the fit program FITTER (Zeiser et al. 2022) was used for this purpose with all parameters fixed except the centre of gravity of both structures.

The concrete results for the individual levels are discussed in the next section.

#### 4. RESULTS

All spectral lines examined are compiled in Table 2, sorted by upper levels under investigation and by wavelength. The wave numbers  $\sigma$  were calculated according to Ritz combination principle from difference between upper and lower level energy. The wavelength in air  $\lambda_{\text{air}}$  were calculated from  $\sigma$  using the refractive index of air according to Ciddor (1996). Energy values and  $J$  values of the upper levels are given according to Chomski et al. (2023), the lower levels according to Wyart et al. (1977); Martin et al. (1978); Kröger et al. (1997).

All lines examined with the LIF method are included in Table 2; if no LIF signal was found, then with the corresponding comment. The lines examined in the FT spectrum were only listed in the table when a signal could be seen at the corresponding position. Exceptions are lines mentioned in Chomski et al. (2023). Such lines were also included in the table even though no signal could be seen at the location in our spectra (with the corresponding comment).

A total of 20 lines were examined with LIF. LIF signal could only be detected for three of these lines. For one out of the three lines, the hfs of the line did not match the expected transition. So in the end, matching LIF lines were only found for two of the levels under investigation.

##### Level 39019.06 $\text{cm}^{-1}$

For this level, two FT lines and one LIF line were found, all of which show clear and distinct structures that support the assumption of the level's existence. The lines are shown in Figure 1.

The simulations for the FT spectrum (Figure 1a and b) are

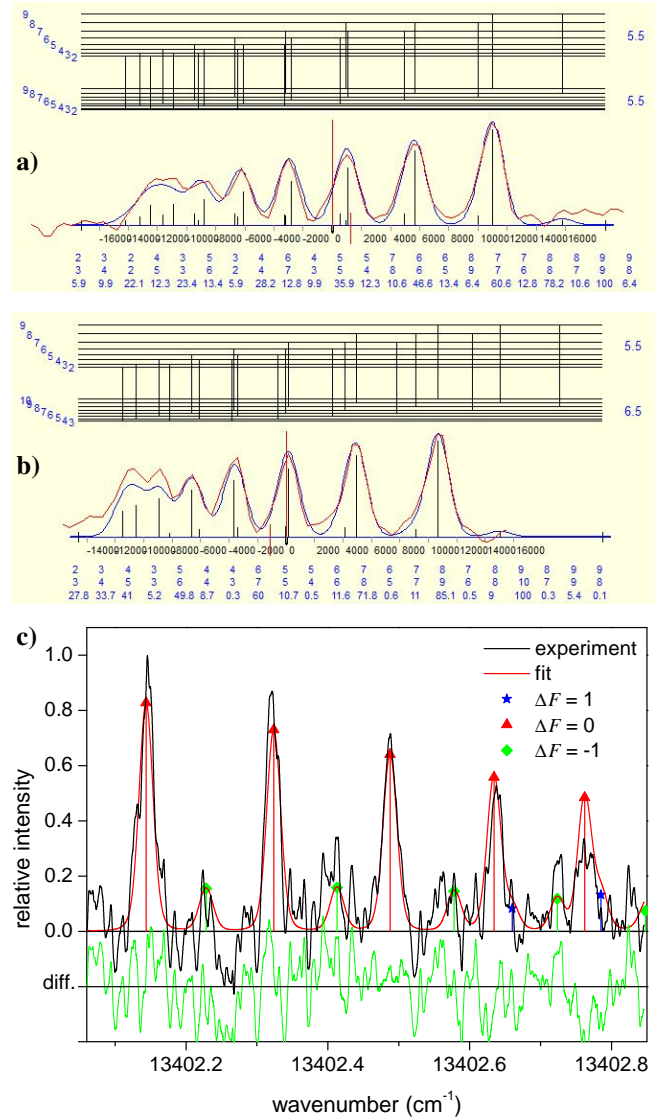


**Figure 1.** Lines including the new odd-parity upper energy level  $E = 39019.06 \text{ cm}^{-1}$ ,  $J = 11/2$ ; a) and b) simulation, and c) fit a) FT-line at  $\lambda_{\text{air}} = 527.327 \text{ nm}$  to the level  $E = 20060.76 \text{ cm}^{-1}$ ,  $J = 11/2$  b) FT-line at  $\lambda_{\text{air}} = 539.653 \text{ nm}$  to the level  $E = 20493.77 \text{ cm}^{-1}$ ,  $J = 13/2$  c) LIF-line at  $\lambda_{\text{air}} = 745.920 \text{ nm}$  to the level  $E = 25616.48 \text{ cm}^{-1}$ ,  $J = 11/2$

screen shots from the program ELEMENTS (Windholz 2016). In the upper part of the representation of the simulations the term scheme with the corresponding transitions is drawn. The  $J$ -values of the levels are indicated on the right-hand edge of the term scheme, and the  $F$ -values of the hfs-sub-levels on the left-hand edge. Below the curve, for each hfs transition the  $F$ -quantum number of the upper and lower hfs-sub-levels and the relative intensity of the transitions are listed one above the other. These data are not in scale to the wavelength axis (which is given in MHz), but corresponds to the occurrence of the transitions (from left to right) in the order term scheme. The

same applies to all other figures of simulations of FT spectra (i.e. Figures 2a, 4c, 5, 6, 7a,b and 8a-c).

In the representation of the fit of the LIF spectrum (Figure 1c) the hfs components are marked by the difference  $\Delta F$  of the  $F$  quantum number of the upper and lower hfs levels. In the lower part the figure, the difference (diff.) between experimental and best-fit curve is given. The same applies to the other figure of fit of the LIF spectrum (i.e. Figure 7c).

The hfs of the line measured with LIF and shown in Figure 1c is wider than the section that can be seen in the Figure. This is because the line is wider than the laser scan range. Although since only a section is visible, the structure of the line clearly fits the expected structure of the transition.

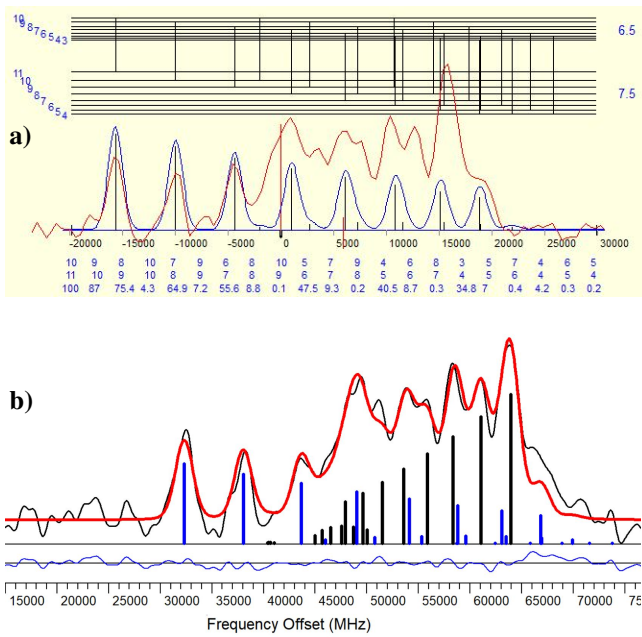


**Figure 2.** FT-Line including the new odd-parity upper energy level  $E = 40438.59 \text{ cm}^{-1}$ ,  $J = 13/2$ ; at  $\lambda_{\text{air}} = 472.421 \text{ nm}$  to the level  $E = 19276.94 \text{ cm}^{-1}$ ,  $J = 15/2$   
 a) simulation, and b) fit considering the blending line

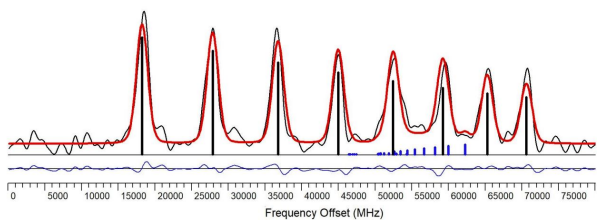


**Figure 3.** Further line including the new odd-parity upper energy level  $E = 40438.59 \text{ cm}^{-1}$ ,  $J = 13/2$ ; FT-line at  $\lambda_{\text{air}} = 557.880 \text{ nm}$  to the level  $E = 22518.55 \text{ cm}^{-1}$ ,  $J = 11/2$ ; fit considering the blending line; line under investigation (blue bars) is only faintly visible under the blending line (black bars)

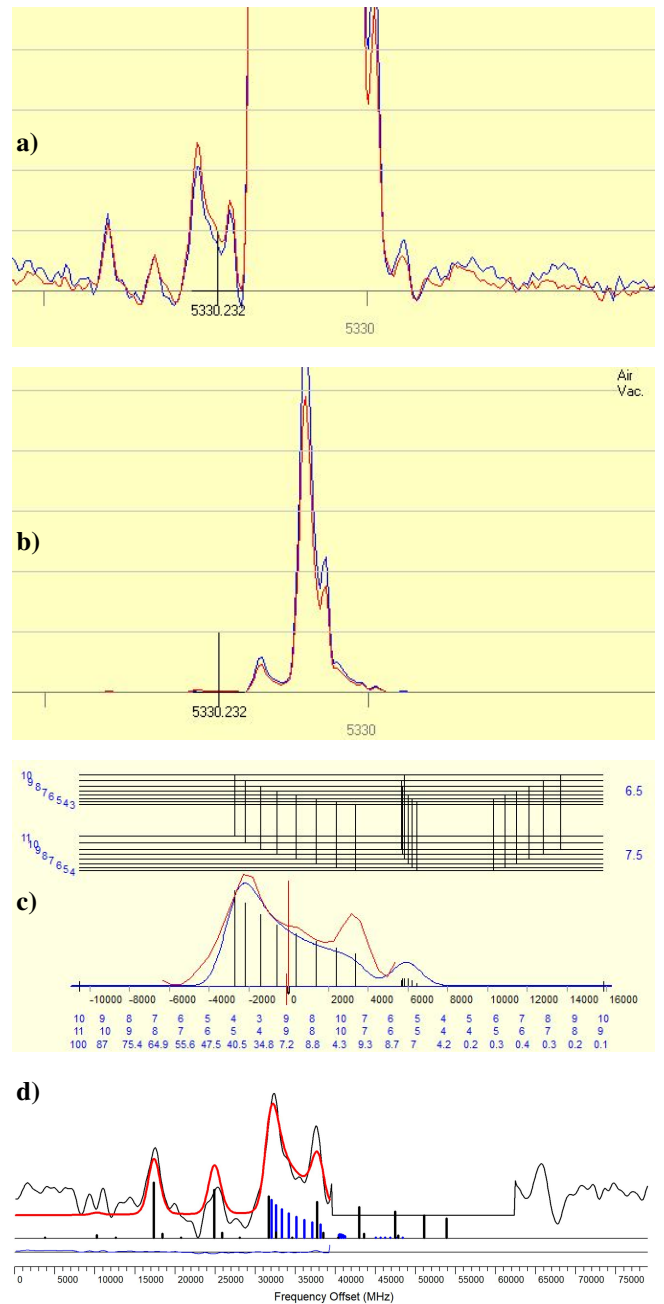


**Figure 4.** FT-Line including the new odd-parity upper energy level  $E = 40438.59 \text{ cm}^{-1}$ ,  $J = 13/2$  at  $\lambda_{\text{air}} = 533.023 \text{ nm}$  to the level  $E = 21682.90 \text{ cm}^{-1}$ ,  $J = 15/2$ ; the line under investigation lies on the left edge of a very strong, well-known line. To illustrate this, in a) and b) the same section is shown with different scales on the y-axis. The vertical black bar marks the position (cog) of the line under investigation.

- a) one graduation mark corresponds to  $S/N$  of 10
- b) one graduation mark corresponds to  $S/N$  of 2560
- c) simulation of a very limited excerpt; only line under investigation
- d) simulation of a slightly wider excerpt, considering the additional weak blending line, whereby the area of the very strong blending line was blanked out

In summary, with these three lines the level  $39019.06 \text{ cm}^{-1}$  could be clearly confirmed.

### Level 40438.59 cm<sup>-1</sup>

For this level, 15 lines have been examined with LIF and not a single one showed a LIF signal. LIF measurements are not yet a proof that the level does not exist nor that it exists.

Additionally we examined all lines to this level in the FT spectrum. Six lines are listed in Table 2. Two of the lines, given by (Chomski et al. 2023) as transition to the level show a hfs which complete differ from the simulated/expected hfs for the investigated transitions. For two other lines given by (Chomski et al. 2023) and for one additional line not mentioned in (Chomski et al. 2023) there is a matching signal in the FT spectrum, but the lines were blended with other lines.

The first line is shown in Figure 2a and b, in 2a a simulation of only the transition under investigation and in 2b a simulation considering the blending line. In Figure 2b, the components of the different lines are marked with vertical bars of different colours (blue and black). The blending line is known (36954.18 cm<sup>-1</sup>,  $J = 13/2 \rightarrow 15792.13$  cm<sup>-1</sup>,  $J = 11/2$ ) and the known hfs constants  $A$  and  $B$  were used for the simulation.

The second line is shown in Figure 3 is weak and blended by a stronger line, which has a broader hfs. Not much could be seen in this case, but it is possible to show in Figure 3, that the disturbance under the strong line could come from the line we are looking for. Here the strong blending line is not classified or unclassifiable, respectively. This means that (at least) one unknown level is involved in the transition. Even without classification, it was possible to achieve an acceptable simulation.

The third line, shown in Figure 4a to d in different representations, lies at the edge of a very strong line, the intensity of which is higher by a factor of more than 500. At the same time the line under investigation is also blended by a second weak but wider splitting line. Figure 4a and b show only the section of the FT spectrum in two different scatterings of the y-axis (without simulation) in order to illustrate the differences in magnitude. The centre of gravity (cog) of the line under investigation is marked by a vertical black bar.

Figure 4c shows only a very small section of the spectrum with a simulation of only the examined line. The match is quite good even though the disturbance of one hfs component of the weak blending line is visible. The weak blending line is known (37623.18 cm<sup>-1</sup>,  $J = 15/2 \rightarrow 18867.54$  cm<sup>-1</sup>,  $J = 13/2$ ) while the strong blending line could not clearly identified. Figure 4d shows a simulation of the examined line together with the weak blending line. The hfs constants  $A$  and  $B$  of both levels of both lines were known and used for the simulation. The area of the strong line was blanked out in this simulation.

A further FT line shown in Figure 5 is observed, but it was very weak and unresolved.

All these lines are not very convincing for proof, thus we recommend further verification for this level.

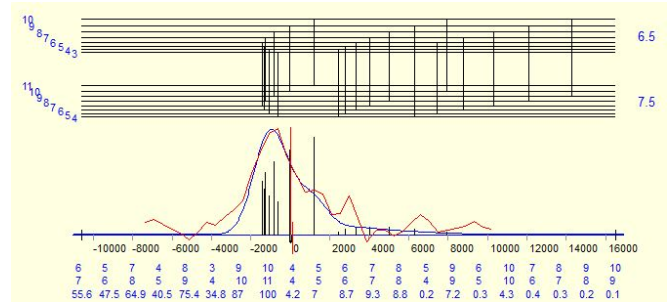


**Figure 5.** Further lines including the new odd-parity upper energy level  $E = 40438.59$  cm<sup>-1</sup>,  $J = 13/2$ ; FT-line at  $\lambda_{\text{air}} = 542.606$  nm to the level  $E = 22014.12$  cm<sup>-1</sup>,  $J = 15/2$

### Level 42189.40 cm<sup>-1</sup>

For this level, five lines have been examined with LIF. None of those showed a LIF signal. The only FT line to this levels found is shown in n Figure 6. This line is not very strong and does not own much structure. Nevertheless, the shape quite clearly fits the transition under investigation. This single line studied is among the lines reported in (Chomski et al. 2023). However, this fact is not useful for reliable confirmation, thus, we recommend further verification for this level.

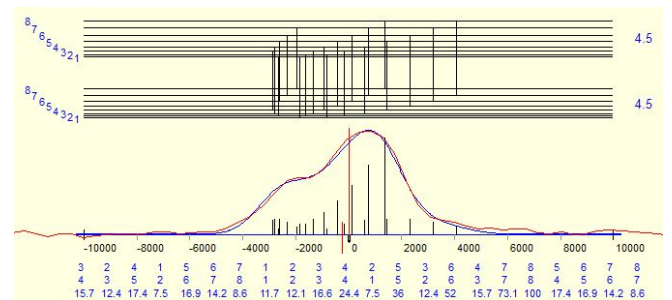


**Figure 6.** FT-line including the new odd-parity upper energy level  $E = 42189.40$  cm<sup>-1</sup>,  $J = 9/2$  at  $\lambda_{\text{air}} = 499.074$  nm to the level  $E = 22157.88$  cm<sup>-1</sup>,  $J = 9/2$ .

### Level 36071.92 cm<sup>-1</sup>

For this level, same as for the first level at 39019.06 cm<sup>-1</sup> two FT lines and one LIF line were found, all of which show clear and distinct structures. The lines are shown in Figure 7. The blends on the left side of the line in Figure 7a and on the right side of Figure 7b do not disturb the clearly recognisable structures. With these three lines the level 36071.92 cm<sup>-1</sup> could be clearly confirmed.

### Level 44283.99 cm<sup>-1</sup>

For this level, there is no theoretical line available that falls within the wavelength range of our laser. Instead, three FT lines were found (see Figure 8). One of the lines is very weak (Figure 8a), and for the other one the splitting is so small that only one

peak can be seen (Figure 8c). The remaining line showed a clear and distinct structure (Figure 8b). The value can therefore be considered as confirmed, however this single line is one among the lines reported in Chomski et al. (2023). Confirmation by a line that is not mentioned in the reference would have been more satisfactory. Thus, we declare the status of this level as “further investigation recommended.”

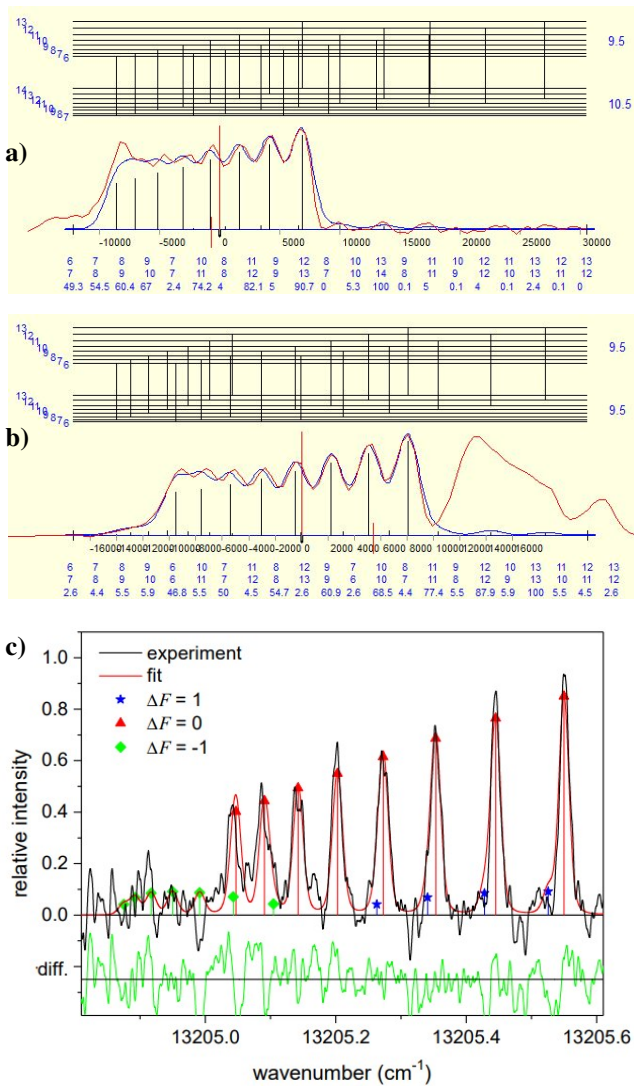


**Figure 7.** Lines including the new odd-parity upper energy level  $E = 36071.92 \text{ cm}^{-1}$ ,  $J = 19/2$ ; a) and b): simulation, and c): fit  
 a) FT-line at  $\lambda_{\text{air}} = 403.933 \text{ nm}$  to the level  $E = 11322.31 \text{ cm}^{-1}$ ,  $J = 21/2$   
 b) FT-line at  $\lambda_{\text{air}} = 410.020 \text{ nm}$  to the level  $E = 11689.77 \text{ cm}^{-1}$ ,  $J = 19/2$   
 c) LIF-line at  $\lambda_{\text{air}} = 757.059 \text{ nm}$  to the level  $E = 22866.55 \text{ cm}^{-1}$ ,  $J = 19/2$ .

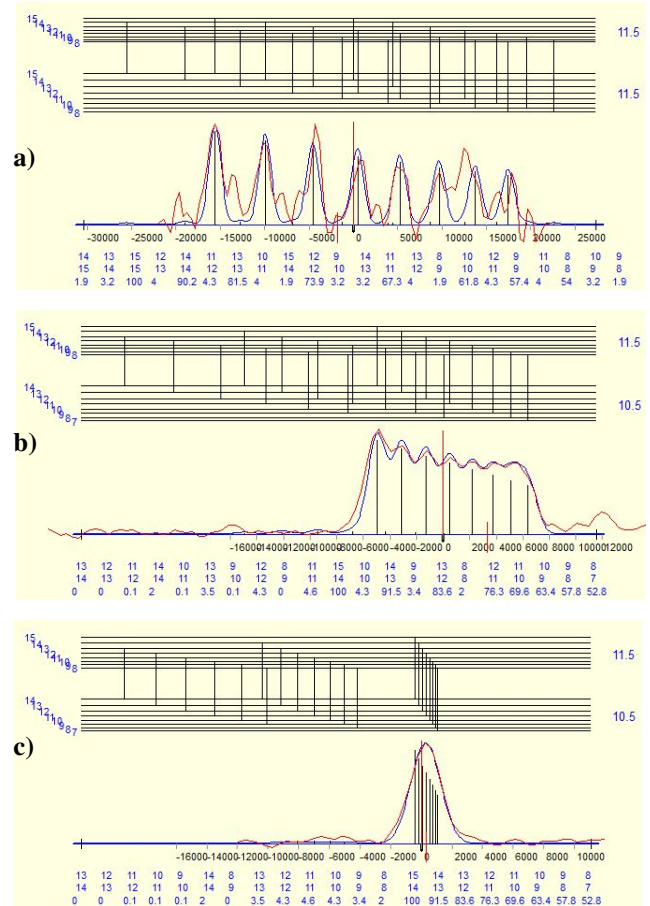


**Figure 8.** Lines including the new odd-parity upper energy level  $E = 44283.99 \text{ cm}^{-1}$ ,  $J = 23/2$  (simulations);  
 a) FT-line at  $\lambda_{\text{air}} = 448.238 \text{ nm}$  to the level  $E = 21980.67 \text{ cm}^{-1}$ ,  $J = 23/2$   
 b) FT-line at  $\lambda_{\text{air}} = 477.940 \text{ nm}$  to the level  $E = 23366.71 \text{ cm}^{-1}$ ,  $J = 21/2$   
 c) FT-line at  $\lambda_{\text{air}} = 510.853 \text{ nm}$  to the level  $E = 24714.34 \text{ cm}^{-1}$ ,  $J = 21/2$

**5. FURTHER REMARKS TO THE WORK OF CHOMSKI ET AL.**

We have noticed, that several hfs constants  $A$  and  $B$  of previously known energy levels presented in Chomski et al. (2023) as measured for the first time have been available in previously published studies. For comparison, these values in previous studies and from Chomski et al. (2023) are given in Table 3.

Also, there is a printing error for the  $J$  value of the level  $20493.40 \text{ cm}^{-1}$ : In the text as well as when reporting the results in Table 3 of Chomski et al. (2023) it is given as  $J = 9/2$ , whereas in Table 2 of the same reference it is given as  $J = 11/2$ . The value of  $J = 11/2$  is correct.

**Table 3.** Hyperfine structure constants  $A$  and  $B$  for the known energy levels of atomic Ho investigated in Chomski et al. (2023), along with the values from previously published studies.

Level			A in MHz		B in MHz		Ref.
$E$ in $\text{cm}^{-1}$	$J$	$p$	from [1]	from ref.	from [1]	from ref.	
20493.40	11/2 *	e	1019.3 (1.4)	1012.5 (0.7)	277 (70)	641 (28)	[2]
18572.28	15/2	o	805.8 (0.8)	808 (4)	1663 (318)	1990 (180)	[3]
40648.25	17/2	e	663.0 (0.8)	660.5 (1.6)	-761 (151)	-750 (80)	[3]
20210.60	21/2	o	1022.2 (1.3)	1021.8 (1.3)	-663 (95)	-600 (90)	[3]

\* Given as  $J = 9/2$  in [1].

[1] Chomski et al. (2023), [2] Stefanska et al. (2018c), [3] Özdalgıç et al. (2019c).

## 6. CONCLUSION

In this study, as a result of examining the five newly found but unconfirmed energy levels by Chomski et al. (2023), two of the examined levels were confirmed beyond doubt. For the other three levels we recommend further verification. The two levels that could be confirmed are those lying below  $40000 \text{ cm}^{-1}$ .

**Peer Review:** Externally peer-reviewed.

**Author Contribution:** Conception/Design of study - Gö. B., S.K.; Data Acquisition - Gü.B., D.B., S.K.B; Data Analysis/Interpretation - Gö. B., I.K.Ö, F.G., D.B.; Drafting Manuscript - Gö. B., S.K.; Critical Revision of Manuscript - I.K.Ö, Gö. B., S.K.B., S.K.; Final Approval and Accountability - S.K., Gö. B.

**Conflict of Interest:** Authors declared no conflict of interest.

**Financial Disclosure:** This work has been supported by the Istanbul University Scientific Research Project via Project No. 39701 and 37896.

## LIST OF AUTHOR ORCIDS

D. Bingöl	<a href="https://orcid.org/0000-0002-1573-319X">https://orcid.org/0000-0002-1573-319X</a>
Gö. Başar	<a href="https://orcid.org/0000-0002-2428-8163">https://orcid.org/0000-0002-2428-8163</a>
Gü. Başar	<a href="https://orcid.org/0000-0002-8133-7590">https://orcid.org/0000-0002-8133-7590</a>
I. K. Öztürk	<a href="https://orcid.org/0000-0002-3664-3388">https://orcid.org/0000-0002-3664-3388</a>
F. Güzelçimen	<a href="https://orcid.org/0000-0001-8453-9975">https://orcid.org/0000-0001-8453-9975</a>
S. K. Barka	<a href="https://orcid.org/0000-0001-5789-1738">https://orcid.org/0000-0001-5789-1738</a>
S. Kröger	<a href="https://orcid.org/0000-0003-4991-9176">https://orcid.org/0000-0003-4991-9176</a>

## REFERENCES

- Al-Labady, N., Özdalgıç, B., Er, A., Güzelçimen, F., Öztürk, I. K., Kröger, S., Kruzins, A., Tamanis, M., Ferber, R., Başar, Gö., 2017, *ApJS*, 228, 16
- Başar, Gö., Al-Labady, N., Özdalgıç, B., Güzelçimen, F., Er, A., Öztürk, I. K., Ak, T., Bilir, S., Tamanis, M., Ferber, R., Kröger, S., 2017, *ApJS*, 228, 17
- Başar, Gö., Başar, Gü., Özdalgıç, B., Öztürk, I.K., Güzelçimen, F., Bingöl, D., Kröger, S., 2020, *JQSRT*, 243, 106809
- Burghardt, B., Buttgenbach, S., Glaeser, N., Harzer, R., Meisel, G., Roski, B., Traber, F., 1982, *ZPhyA*, 307, 193
- Childs, W.J., Cok, D.R., Goodman, L.S., 1983, *JOSA*, 73, 151
- Ciddor, P. E., 1996, *ApOpt*, 35, 1566
- Chomski, M., Furmann, B., Ruczkowski, J., Suski, M., Stefanska, D., 2021, *JQSRT*, 274, 107865
- Chomski, M., Suski, M., Wilman, S., Furmann, B., Ruczkowski, J., Stefanska, D., 2022, *JQSRT*, 279, 108045
- Chomski, M., Furmann, B., Suski, M., Głowacki, P., Stefanska, D., Mieloch S., 2023, *JQSRT*, 297, 108480
- Elantkowska, M., Ruczkowski, J., Sikorski A., Wilman, S., 2019, *JQSRT*, 237, 106642
- Furmann, B., Stefanska, D., Suski, M., Wilman, S., 2018, *JQSRT*, 219, 117
- Goodman, L.S., Schlüpmann, K., 1964, *ZPhy*, 178, 235
- Kröger, S., Wyart, J. F., Luc, P., 1997, *PhyS*, 55, 579
- Kröger, S., Windholz, L., Başar, Gö., 2023, *PARep*, 2023, 1, 32
- Martin, W. C., Zalubas, R., Hagan, L., 1978, *Atomic Energy Levels - The Rare-Earth Elements*, National Bureau of Standards, NSRDS-NBS, 60, 422
- Merzyn, G., Penselin, S., Wolber, G., 1972, *ZPhy*, 252, 412
- Özdalgıç, B., Güzelçimen, F., Öztürk I. K., Kröger, S., Kruzins, A., Tamanis, M., Ferber, R., Başar, Gö., 2019a, *ApJS*, 240, 27
- Özdalgıç, B., Başar, Gö., Güzelçimen, F., Öztürk I. K., Ak, T., Bilir, S., Tamanis, M., Ferber R., Kröger, S., 2019b, *ApJS*, 240, 28
- Özdalgıç, B., Başar, Gö., Kröger, S., 2019c, *ApJS*, 244, 41
- Reddy, M.N., Ahmad, S.A., Rao, G.N., 1992, *JOSAB*, 9, 22
- Snedden, C., Lawler, J. E., Cowan, J. J., et al., 2009, *ApJS*, 182, 80
- Stefanska, D., Furmann, B., 2018a, *JQSRT*, 206, 286
- Stefanska, D., Ruczkowski, J., Elantkowska, M., Furmann, B., 2018b, *JQSRT*, 209, 180
- Stefanska, D., Furmann, B., Głowacki, P., 2018c, *JQSRT*, 213, 159
- Stone, N.J., 2005, *ADNDT*, 90, 75
- Windholz, L., Guthöhrlein G.H., 2003, *PhST*, 105, 55
- Windholz, L., 2016, *PhyS*, 91, 114003
- Wyart, J.F., Camus, P., Verges, J., 1977, *PhyBC*, 92, 377
- Zeiser, A., Kröger, S., Pooyan-Weis, L., Windholz, L., Guthöhrlein, G., 2022, *JQSRT*, 290, 108294